

Approaches to liver tumors



Dr. Fuminori Moriyasu, MD., Ph. D.
Professor
Department of Gastroenterology and Hepatology
Tokyo Medical University
Tokyo, Japan

Introduction

Ultrasound elastography, which is now also widely employed for the assessment of liver diseases, is categorized into two types: strain elastography, which evaluates strain in response to pressure, and shear wave elastography, which measures the propagation velocity of shear waves. In shear wave velocity measurements, shear waves are generated by applying mechanical vibration or pressure or by applying acoustic pressure. Shear Wave Elastography (SWE), which has been developed by Toshiba Medical Systems Corporation (Otawara, Tochigi, Japan), employs the latter method and also allows the propagation velocities of shear waves to be quantified and mapped.

In this paper, I would like to discuss the SWE approach to liver tumors, including the differential diagnosis of tumors and the applications of SWE in local treatment.

Features and usefulness of SWE

SWE includes a display mode in which the shear wave arrival times are shown as contour lines, permitting the reliability of the acquired elastography information to be verified (Fig. 1).

For example, if distorted contour lines are observed in deep regions, it indicates that reliable information cannot be obtained. Since SWE does not require the application of manual compression, patients with ascites can also be examined. By setting ROIs of the desired size in the color map, the shear wave propagation velocity can be measured quantitatively.

The measured shear wave propagation velocity (m/s) is converted to elasticity (kPa) using the following formula:

$$E = 3 \cdot \rho \cdot V^2$$

where E is elasticity (kPa), ρ is density, and V is the shear wave propagation velocity (m/s)

However, the shear wave propagation velocity is strongly influenced by the elasticity and is also affected

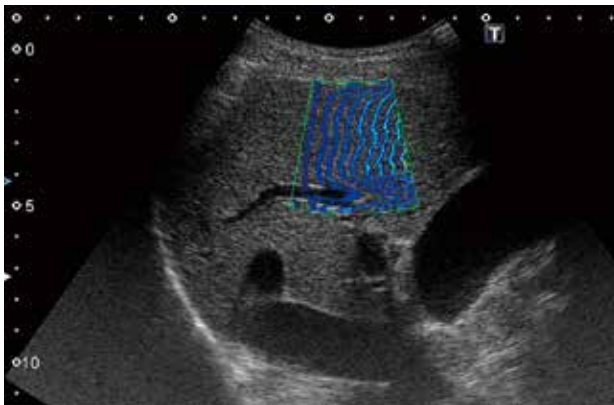


Figure 1. Shear wave arrival time contour display.

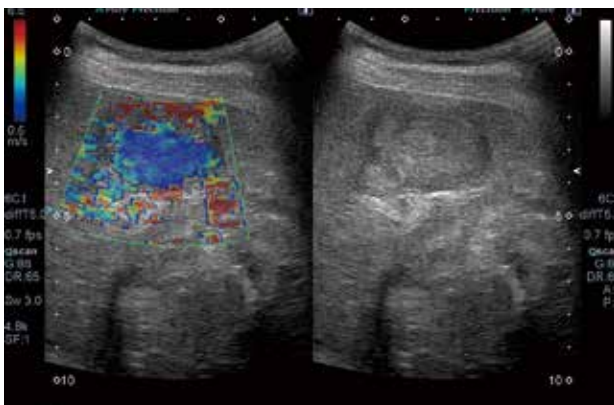


Figure 2. Case 1: SWE color map image.

by the viscosity (Pa·s), particularly in the liver. The viscosity affects the physical properties of the tissues, especially in inflammatory diseases, and is considered to affect the physical properties of tissues in many tumorous conditions as well.

Elasticity is the degree of expansion or contraction (for example, a spring that is compressed with a certain amount of force), while viscosity involves velocity and time (for example, a gas damper on a door). In other words, an object contracts more quickly when it is subjected to a larger force and contracts more slowly when it is subjected to a smaller force. In order to clearly understand the shear wave propagation velocity, the factors of elasticity and viscosity must be taken into consideration.

Applications of SWE in the diagnosis of liver diseases

Applications in diffuse liver diseases

The most common application of SWE in liver diseases is the diagnosis of diffuse liver diseases. In hepatic fibrosis and acute hepatitis, the viscosity increases due to inflammation, cellular necrosis, cellular infiltration, edema, and various other factors, and the shear wave propagation velocity is therefore considered to be significantly faster. Fat deposition is also thought to affect the shear wave propagation velocity, although the applications of SWE in fatty liver and non-alcoholic steatohepatitis (NASH) are currently being actively discussed. For liver tumors, SWE is very useful not only for differential diagnosis but also for assessing the effects of local treatment. This is an important aspect of SWE.

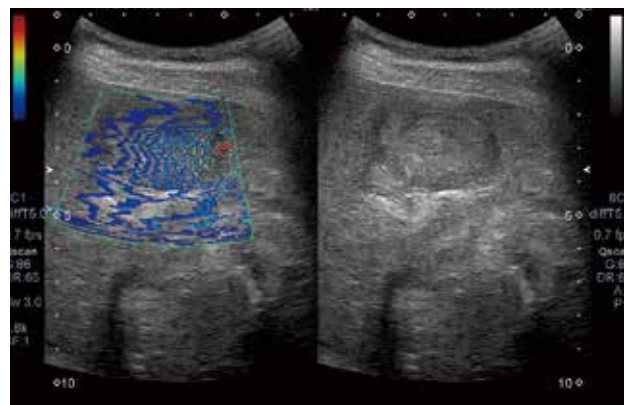


Figure 3. Case 1: Arrival time contour display of the image shown in Figure 2.

The density of the contour lines is higher inside the tumor than in the surrounding cirrhotic areas, indicating that the SW propagation velocity is slower.

Applications in liver tumors

Case 1 is a patient with a large hepatocellular carcinoma (HCC) that appears as a cluster of multiple massive nodules. In the SWE color map image (Fig. 2), there are areas where signals are missing and the reliability is questionable. In shear wave arrival time contour display mode (Fig. 3), however, it can be confirmed that the shear waves propagate without discontinuities, and the map image can therefore be used for the assessment of tissue stiffness.

It is said that SWE may not be useful for assessing the tissue stiffness of complex structures in which the tissues exhibit variation on a fine scale. However, for example, if a wooden post is standing in the path of an ocean wave, the wave pattern on the water surface is disturbed and shows complex movement, but this does not mean that the wave is not traveling. In other words, the disturbed wave pattern represents an abnormal complex state. How such tissue structures should be displayed in SWE is a future challenge. When this challenge has been overcome, it is expected that SWE will become a powerful diagnostic tool for the assessment of tumorous liver diseases.

Case 2 is a patient with a 1-cm HCC that is visualized as a hypoechoic area in B-mode images. In SWE, the tumor is depicted as an area that is stiffer than the surrounding tissues, and in arrival time contour display mode, the shear wave is clearly seen to travel faster in the hypoechoic area (Fig. 4). When ROIs were set and the elasticity was measured, the elasticity in the area of the tumor was 38.8 kPa, which was substantially higher than in the surrounding area, where the elasticity was 18.2 kPa (Fig. 6). This case was diagnosed as moderately to poorly differentiated HCC based on pathologic examination of a biopsy specimen. Thus, quantification using SWE makes it

possible to perform comparison between patients as well as between tumors.

It has been reported that elastography is not suitable for the differential diagnosis of focal nodular hyperplasia (FNH), hemangioma, HCC, and metastatic liver cancer.¹⁾ However, when we performed evaluation for only HCC, comparison of the shear wave propagation velocities between well differentiated HCC, moderately differentiated HCC, and poorly differentiated HCC showed that the stiffness was significantly higher in poorly differentiated HCC than in the other types (Fig. 5). This finding suggests that SWE may also be useful for evaluating the degree of malignancy and assessing tissue characteristics in tumorous diseases.

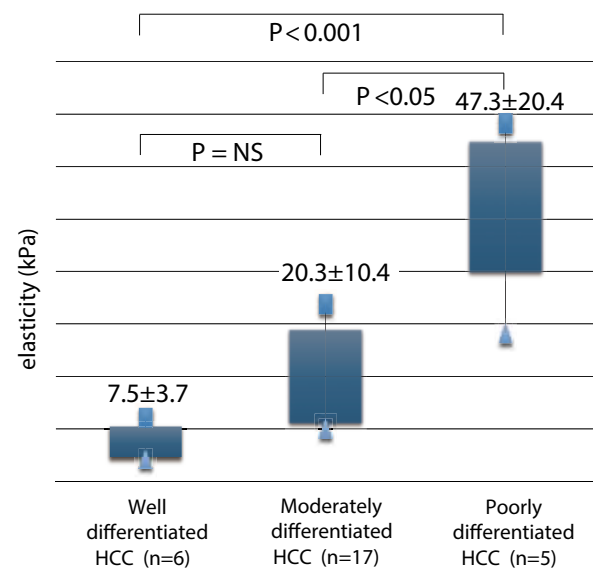


Figure 5. Case 2: Quantitative assessment of tumor elasticity.

The result of elasticity measurement in the ROIs indicates that the tumor is stiffer (38.8 kPa) than the cirrhotic area outside the tumor (18.2 kPa).

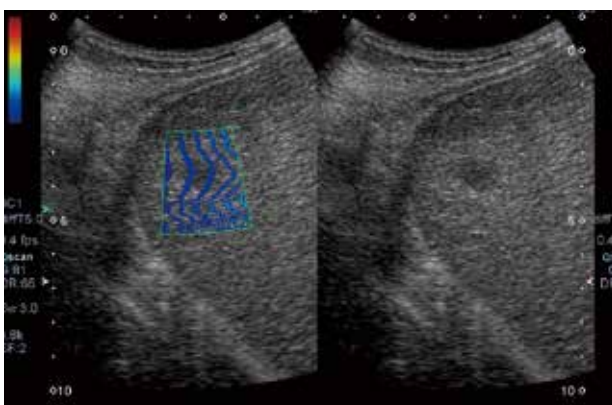


Figure 4. Case 2: Arrival time contour display.

It is clearly seen that the SW propagation velocity is faster (the tissue is stiffer) in the tumor than in the surrounding areas. This case was diagnosed as a moderately to poorly differentiated HCC based on pathological examination of a biopsy specimen.

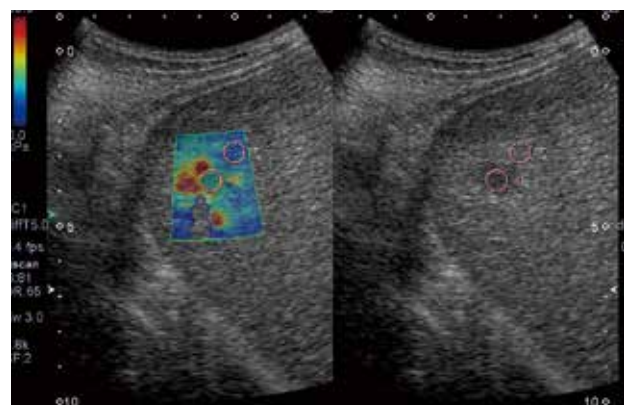


Figure 6. Quantification of the degree of tissue differentiation and elasticity of HCC.

Assessment of the effects of local treatment

Applications in the assessment of treatment effects following irreversible electroporation (IRE)

Recently, ultrasound elastography has been increasingly employed to support local treatment procedures and to assess treatment effects, in addition to diagnosis. In particular, ultrasound elastography is expected to be useful for assessing the effects of the newly developed treatment technique, IRE (NanoKnife™, AngioDynamics, Inc., Latham, NY, USA). In IRE procedures, high-voltage (3000 V) direct current is applied across multiple 19G needle electrodes to create small irreversible perforations in the cell membrane. This induces apoptosis in the cancer cells, leading to cell death.

Following radiofrequency ablation (RFA) procedures, the cells and tissues appear white as a result of the denaturation of proteins. Following IRE procedures, which do not cause a local temperature increase, the tissues appear reddish brown due to severe blood congestion. At the cellular tissue level, RFA causes almost no morphological changes except for slight hypochromasia, but the high temperatures generated during the procedure disrupt cellular functions, destroy tissue structures, and interrupt blood flow.

Following IRE, on the other hand, cells that have lost their nuclei are seen in images, the number of cells is reduced, and the extracellular space is filled with red cells in the sinusoids. Apoptotic nuclear degeneration is also observed. IRE destroys the cells only. It does not destroy the fibrous tissues, and as a result, the vascular structure is maintained. The vascular endothelial cells undergo apoptotic degeneration, but they are thought to regenerate within 48 hours, and the vascular smooth muscle cells are thought to regenerate in approximately 2 weeks. Such conservation of tissue structure is also observed in the pancreatic duct, bile ducts, urinary tract,

gastrointestinal tract, and gallbladder. It is therefore considered that IRE can destroy cancer cells invading blood vessels, and this method is expected to be useful for the treatment of various types of cancers in the future. In addition, due to the heat sink effect, RFA cannot induce sufficient heating in tumors that are located close to large vessels, and there is a high risk of recurrence. IRE does not suffer from this limitation because it is not a heat-dependent technique.

Second case treated by IRE in Japan

IRE has been used to treat more than 3500 cases in Europe and the United States. In Japan, however, it is still in the clinical research phase. The first successful IRE procedure in Japan was performed at our institution in February 2014. The second case treated by IRE at our institution is presented below. In this case, RFA was used to treat a hypervascular nodule measuring approximately 2 cm, but a sufficient area could not be coagulated due to the presence of nearby blood vessels. Recurrence was confirmed 8 months after RFA, and IRE was performed.

Based on preoperative simulation using 3D images, four needles were inserted via an intercostal space. A shot of high-voltage electric current was applied every heartbeat in synchronization with the ECG waveform up to a total of 180 shots. During the procedure, the positions of the needle tips were monitored using the needle navigation system of the ultrasound system (Fig. 7). A post-treatment EOB-MR image showed that a sufficient area was treated as compared with RFA performed 8 months previously.

As discussed above, IRE can be used to treat cancers located near the digestive tract or gallbladder as well as cancers close to large blood vessels or even within blood vessels. This method is therefore expected to replace many types of treatment for liver cancer in the future (Fig. 8).

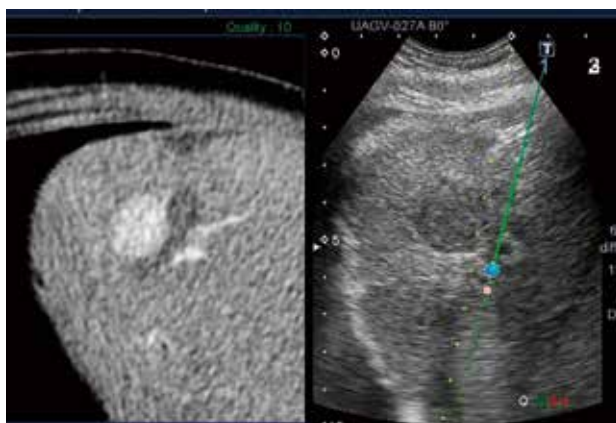


Figure 7. Fusion image and needle navigation image in the second case treated by IRE in Japan.

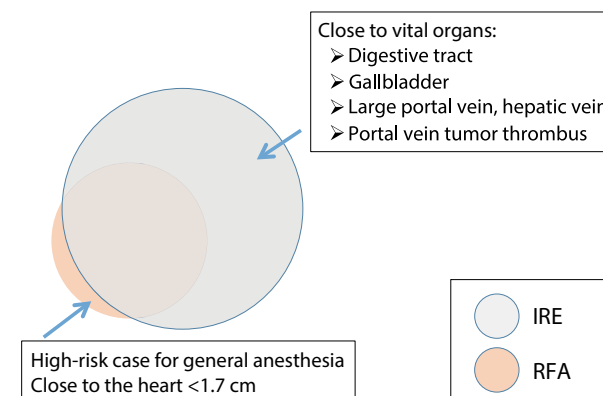


Figure 8. Applications of RFA and IRE in liver cancer.

One of the current challenges in IRE is that it is difficult to confirm the extent of treatment, especially during the procedure itself. To address this problem, ultrasound imaging technologies, and especially elastography, are expected to be useful.

In contrast ultrasound imaging employing Sonazoid, areas of reduced Kupffer cell function are clearly visualized in the Kupffer phase (Fig. 9).

In cases in which blood flow within the tumor is absent, the blood flow in surrounding areas can be evaluated by repeating the injection of contrast medium. It is therefore expected that the extent of treatment can be assessed based on the degree of blood flow.

SWE can be used to assess the extent of treatment without the need to administer contrast medium (Fig. 10). It is also possible to confirm the reliability of SWE using arrival time contour display mode (Fig. 11).

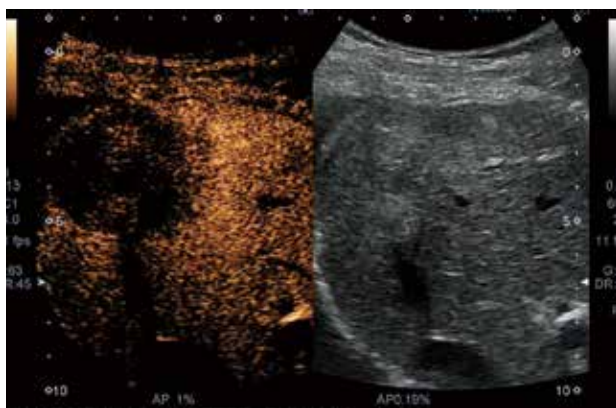


Figure 9. Assessment of the extent of IRE treatment in the Kupffer phase of contrast ultrasound imaging.

The extent of treatment cannot be confirmed at all in the B-mode image. In the Kupffer-phase image obtained by contrast ultrasound using Sonazoid, the extent of treatment can be clearly seen, which is thought to be because the phagocytic activity of the Kupffer cells is lost following IRE.

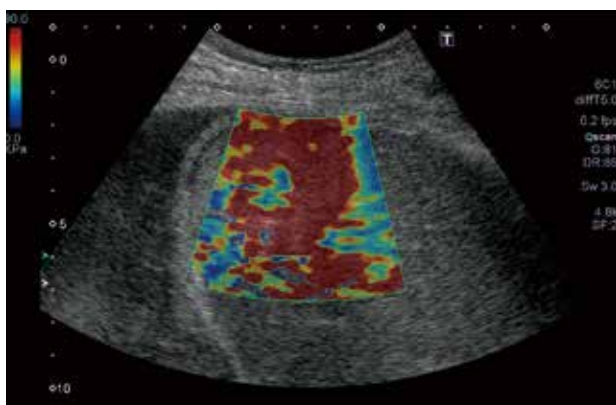


Figure 10. Assessment of the extent of IRE treatment using SWE.

The treated area is displayed in red, indicating that the tissues are stiff. It is considered that the viscosity in this area is increased. In comparison, the tumor is displayed as soft tissue.

It is not easy to evaluate the changes in tissue characteristics and physical properties following an IRE procedure. However, SWE, which permits noninvasive evaluation by simply applying ultrasound signals, is expected to play an important role in the assessment of local treatment in the future.

Usefulness of needle navigation in interventional ultrasound

Needle navigation, is a promising system for use in ultrasound-guided interventional procedures, which have become the mainstream for the treatment of liver tumors in Asia. A magnetic sensor mounted to the base of the puncture needle (Fig. 12) detects the position of the needle tip and displays a blue dot ● at the corresponding



Figure 11. Arrival time contour display mode of the image shown in Figure 10.



a: Needle navigation system

b: Multi-needle navigation

Figure 12. Needle navigation system.

The position of the needle tip is detected by a magnetic sensor mounted to the base of the needle and is displayed in the image (a). When a magnetic sensor is mounted to each of the three needles as well as to the transducer, the three-dimensional positional relationships between the tomographic ultrasound plane and the three needles are detected and displayed (b).

location in the ultrasound image (Fig. 13). This is very useful for confirming the position of the needle tip and ensuring that the needle is accurately advanced to the target.

Toshiba Medical Systems Corporation is also developing the Needle Enhancement function, which improves depiction of the needle in the ultrasound image (Fig. 14). In this function, the needle signals are enhanced by changing the direction of the ultrasound beam, allowing the needle to be more clearly visualized on the screen. Needle Enhancement is also expected to be widely employed in clinical practice.

The needle navigation system is also helpful in cases in which the needle tip is obscured by the gases that are generated by tissues during RFA procedures (Fig. 15). In

addition, multi-needle tracking is required for recently introduced ultrasound interventions such as IRE and RFA procedures employing two or more needles. Toshiba Medical Systems Corporation is also developing an advanced needle navigation system in which a sensor is mounted to each of three needles, allowing the positions of the three needle tips to be monitored simultaneously (Fig. 12b). This system is expected to be extremely useful for advancing multiple needles with high precision during the treatment of relatively large liver tumors (Fig. 16).

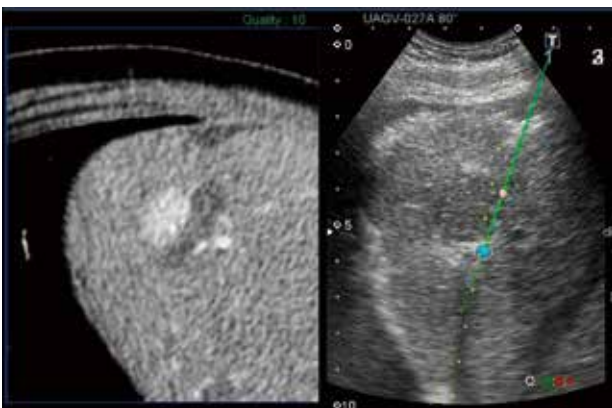


Figure 13. Needle navigation images.

Even when the needle tip is not visible in the image, the position of the needle tip can be estimated (indicated by a blue dot ●).

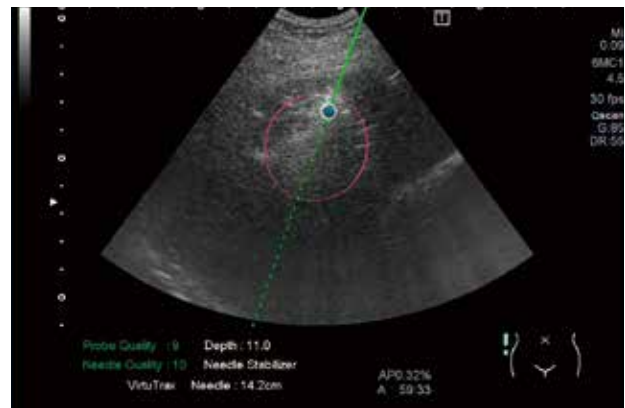


Figure 15. Display of the estimated ablation range of RFA using the needle navigation system.

The blue dot ● indicates the needle tip and the pink ellipse indicates the estimated ablation range.



Figure 14. Needle enhancement display of the needle navigation system (WIP).

Compared with a conventional B-mode image, visualization of the needle is improved in the image acquired with needle enhancement.

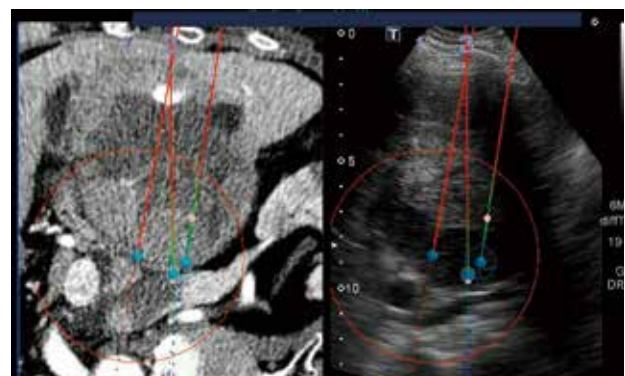


Figure 16. Needle navigation image and corresponding multi-needle tracking image (WIP).

Three needles are displayed by multi-needle tracking, and the needle positions within the corresponding CT volume data are indicated in fusion imaging.

Conclusion

SWE and the needle navigation system are indispensable technologies not only for diagnosis but also for monitoring and assessing local treatment. These new technologies are expected to undergo further development and to gain widespread clinical acceptance in the future.

References

- 1) Yu H, Wilson SR. Differentiation of benign from malignant liver masses with Acoustic Radiation Force Impulse technique. *Ultrasound Quarterly* 2011; 27 (4): 217-223.

CANON MEDICAL SYSTEMS CORPORATION

<https://global.medical.canon>

©Canon Medical Systems Corporation 2018. All rights reserved.
Design and specifications are subject to change without notice.
MOIUS0075EAA 2018-05 CMSC/SO/Printed in Japan

Canon Medical Systems Corporation meets internationally recognized standards for Quality Management System ISO 9001, ISO 13485. Canon Medical Systems Corporation meets the Environmental Management System standard ISO 14001.

Made for Life is trademark of Canon Medical Systems Corporation.

Toshiba Medical has changed its company name to Canon Medical Systems Corporation as of January 4th, 2018.
This document was created prior to the name change and therefore the former company name may still be referred to within the document.

Made For life